Hydrodynamics Related to Shipwreck Taphonomy

Sean M. Kery, Jillana Stauffer
CSC Advanced Marine Center

Abstract

When a shipwreck and objects in the associated debris field land on the seabed, they continue to be acted on by currents and benthic storms that can result in changes to the position, orientations and dispersion. In shallower waters, ocean storm waves and long period swells can cause strong oscillatory water motions to act on the objects. This paper describes a number of cases where the underwater archeological record shows evidence of these changes, and shows how such cases may be modeled using modern COTS software. The technical approach described in this paper shows how the different specialties of naval architecture, oceanography, ocean engineering, sediment transport, hydrodynamics and underwater archaeology can be usefully combined under the umbrella specialty of marine forensics.

The phenomenologies associated with freefall in the water column, bottom impact, and then the impact of various post deposition events and processes are modeled for several historic wrecks and the process and results are illustrated. The differential action of storm waves and how to calculate their frequency of occurrence at a specific depth will be described. The sediment transport like action that can re-suspend objects and or tumble them across the seabed will be described and modeled for typical objects. The action of strong oscillating water motions can expedite a wreck's breakup. Scour and erosion corrosion at the water-to-sediment interface have been implicated in specific damage to some historic wrecks.

Lastly, the implications to modern search and rescue and to the research of historic wrecks will be discussed.

Introduction

Underwater Archaeology pioneered by Bass (1975 & 2005), Throckmorton (1987), and many others began in the 1960's when the tools that enabled it were first available. Today it is a mature sub-field of archaeology. Other investigators, such as Steffy (1994) and Tanner (2013) have developed techniques for re-engineering the structure of ancient ships and in some cases modern day replicas that can be sailed again. This paper describes the use of naval architecture based marine forensic techniques to model how a shipwreck arrives at the seabed and how the marine environment continues to act on it to produce the debris field as found at a later date.

Shipwreck behavior in the water column

When a vessel leaves the surface for whatever reason and falls and flutters to the seabed, its behavior in the water column is a complicated summation of weight, buoyancy, drag and lift forces and moments, which are rate, direction and time dependent.

Vessels in very shallow water such as the *Costa Concordia* have very little time in the water column in which to flutter and change their orientation. Vessels in somewhat deeper water depths such as the USS *Monitor, Andria Doria* or the *Lusitania* reach the bottom in more or less the orientation at which they left the surface. In deep waters, the motions can be much more complicated. The DKM *Bismarck* left the surface upside down and bow last, but hit the

978-0-933957-43-5 ©2015 MTS

seabed bow first and upright. Cameron et al, (2008) The RMS *Titanic* broke at or near the surface and the two major parts landed a considerable distance apart with a significant debris field scattered over a broad area.

The rate of descent can be calculated as the terminal velocity whereby the weight acting downwards less the buoyancy acting upwards is balanced against the drag induced by the velocity. With some algebraic manipulation of the standard drag equation, this comes out as:

$$V_{terminal} = \sqrt{\frac{2(Weight - Buoyancy)}{roe * Cd * Area}}$$

Where roe is the fluid density, Cd is the drag coefficient and the Area is defined differently depending on how the drag coefficients were derived from empirical data. (Hoerner 1965, Hoerner & Borst 1975, Pattison et al 1977)

While the weight during freefall is reasonably constant, pieces that fall or float off, or that move around due to motions or free surface effects, can make weight and the 3 dimensional center of gravity a dynamic quantities.

Buoyancy suffers the same perturbing effects as weight but is also impacted by rapidly increasing hydrostatic pressure with depth. Due to pressure increases, air pockets compress adiabatically or leak out, if they are surrounded by sufficient structure, implode catastrophically when the structure's crush depth is exceeded. (Faulkner 1998)

On wooden or composite vessels, the hollow and air filled material is partially crushed and partially flooded, as water wicks along fibers and into the interstitial spaces and pores. This partial crushing, as the object descends faster than the water can wick in, is suggested to cause significant morphological changes that may significantly reduce structural integrity on the way down. Pressure treated wood used in modern outdoor construction is 10 to 20% weaker than the parent lumber, so at least that much strength is lost. This also means that when the vessel comes to rest, the residual stresses in the materials, and their buoyancy may continue to change over the first few hours to weeks as the materials reach saturation.

The authors are not aware of any studies where samples of different woods typically used in shipbuilding, have been systematically subjected to different rates of increasing hydrostatic pressure to observe and quantify these effects. This could be accomplished relatively easily in a shore side pressure chamber.

The water density varies with temperature, salinity and pressure over the water column, and in some cases this relatively small variation can be critically important, such as when the weight and buoyancy are nearly balanced. For objects ballasted to near neutral buoyancy, such as a Remotely Operated Vehicle (ROV), a small change in the fluid density with depth may reduce the terminal velocity to near zero.

The lower part of a vessels hull that is normally submerged in water is optimized for low drag in the fore and aft direction. No attempt is made to minimize the drag in the transverse or vertical directions because the vessel does not normally travel in those directions.

Water is about 700 times denser than air, therefore objects traveling through air only have about 1/700th the amount of drag as when they are submerged in water. During normal operations, the drag of the upper parts of a vessel can have a lot more drag area with minimal resulting drag force or loss of fuel economy and these are rarely considered for drag reduction.

The different parts of a ships upper hull, superstructure, and rigging have complicated shadowing effects and very different drag coefficients for different parts.

Parts such as railings, smokestacks or rigging are very different in size such that they experience flow at different Reynolds and Strouhal Numbers. The normal drag coefficient of circular cylinders such as ropes, masts, railings and smokestacks, can vary from 1.2 to as high as 4.0, when vortex induced vibration "locks on". However the lock-on phenomenon is very sensitive to the angle the cylinder makes to the flow direction and the stiffness / tension of the cylinder.

The topside drag due to all of the shapes for any typical vessel is typically much greater than the drag of the parts that are normally submerged. For ships such as sailing vessels, the drag of the top hamper can be many times the drag of the lower hull. While these upper portions of a vessel are typically not considered in drag calculations, when modeling a shipwreck's movement in the water these can be crucial components.

As any object flutters and tumbles in the water column, the areas exposed to the flow, and the way that shedding vortices are created, changes continually. This in turn changes the three dimensional path of motion and the relative velocities acting on any of the various parts that are exposed to the flow.

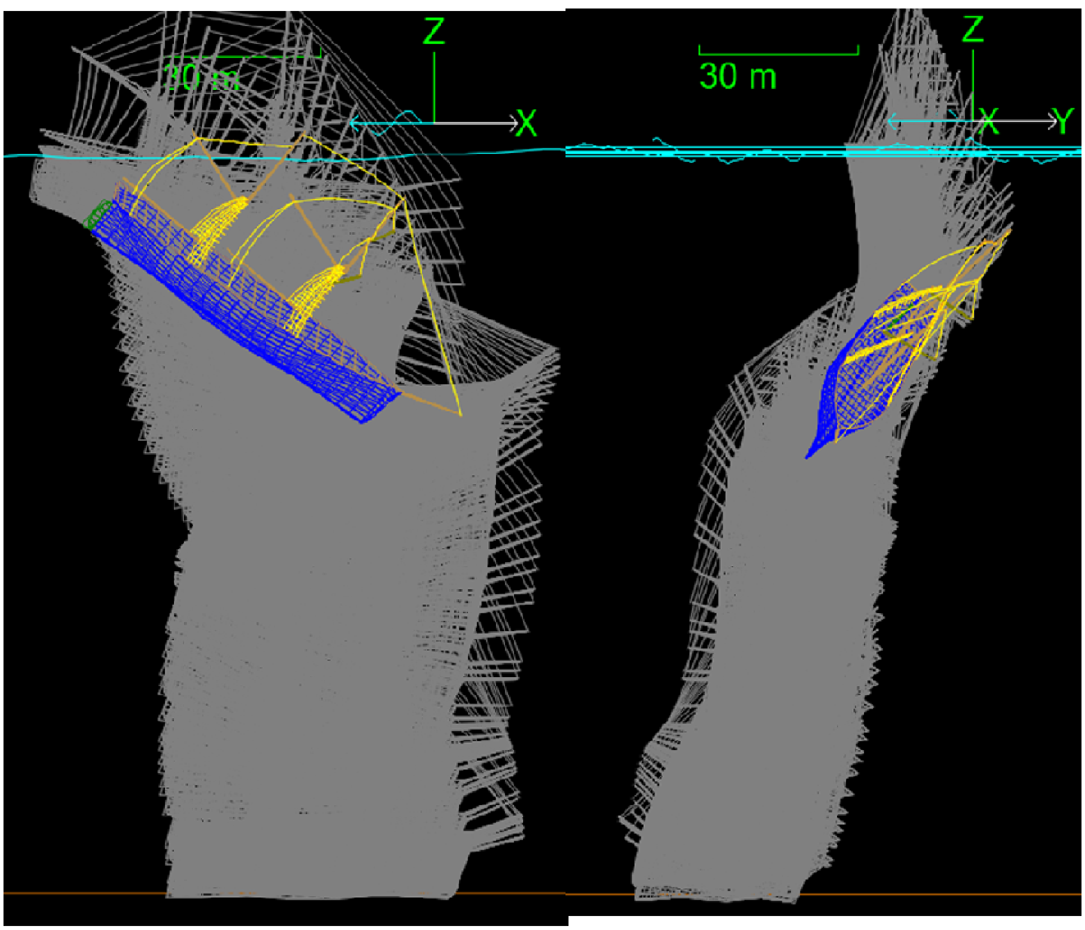

Figure 1: Two views of Topsail Schooner Sinking in Orcaflex Model (Kery 2015)

The authors have developed a methodology whereby all of the factors discussed can be studied acting simultaneously using the Commercial Off the Shelf (COTS) OrcaFlex software package. (Orcina.com) (Kery 2015 (2)) Among the critical inputs to these analyses are the weights and three dimensional centers of buoyancy and gravity for the vessel in the sinking condition. (Kery 2015 (1))

Using this methodology, Figure 1 shows two views of a generic topsail schooner sinking intact in storm waves. The cause of the sinking is not relevant to the analyses discussed in this paper and is not discussed. The weights and buoyancy distributions of the hull and top hamper were calculated in meticulous detail. The drag areas and coefficients are modeled as accurately as feasible for this illustration level analysis. The only practical limit on the fidelity of the model is how much time the modeler is willing to expend developing and inputting the details.

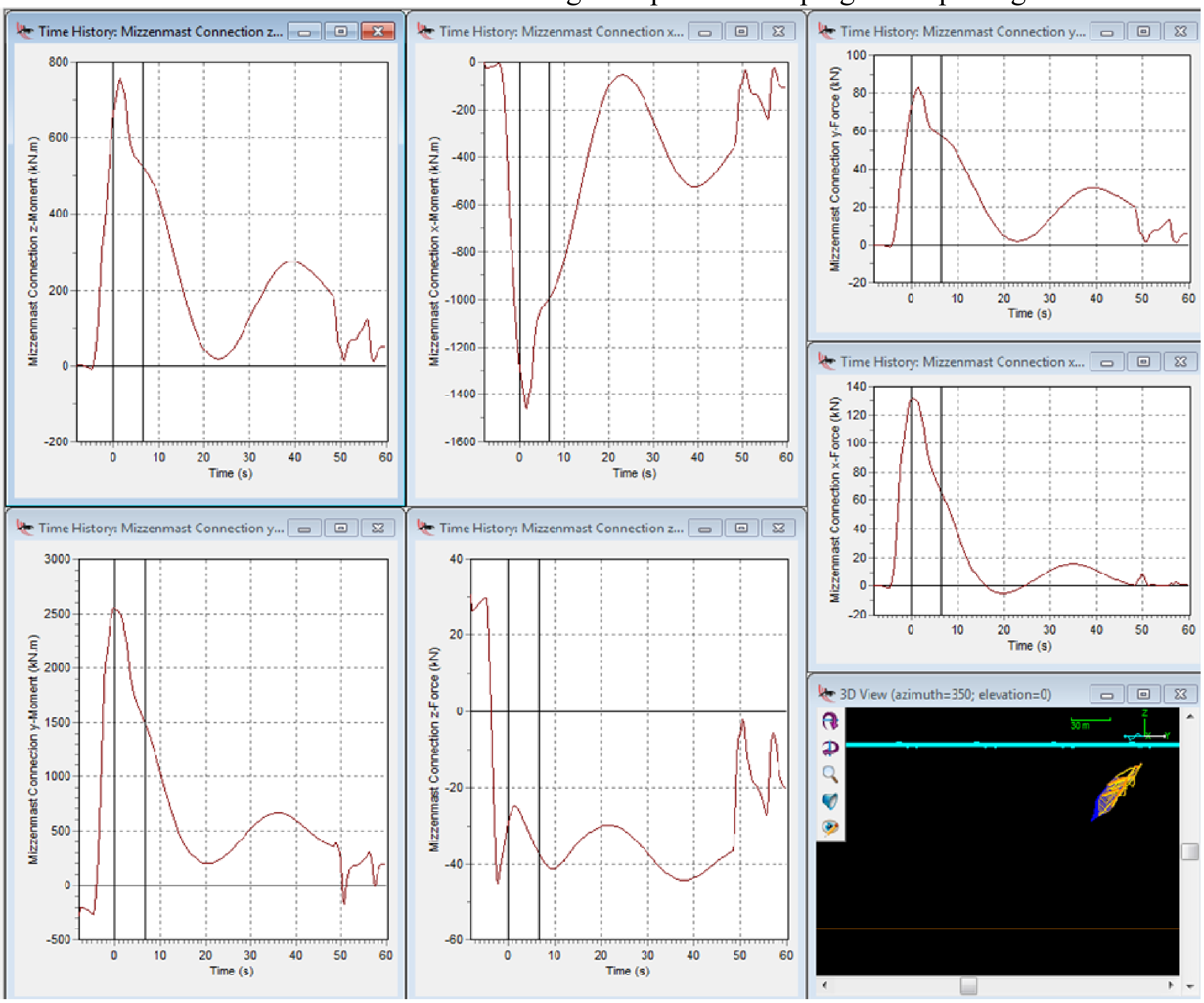

Figure 2: Forces and Moments Acting on Mizzenmast During Freefall.

Figure 2, shows some of the many results that can be extracted as time series in excel from the program. Further study may show that at some point the forces or moments exceeded the strength of the mast(s) or specific lines in the rigging at some point in the descent. At that point, some limited facility exists in the program to repeat the run with user specified components failing at a maximum tension or at a specific instant in time.

Bottom Impact

An object freefalling in the water column eventually encounters the bottom. The seabed material condition and shape, and the object's susceptibility to elastic and plastic deformation have effects on the forces and moments that result. This is similar to any other form of impact analyses but with additional complications due to the presence of dense and nearly incompressible fluid. In addition to the important characteristics of an impact on land, such an as automobile crash, analyses of seafloor impacts include drag and added mass terms.

Added mass includes the water trapped in the object as well as water traveling with it entrained in the boundary layer and wake. The added mass is typically the volume of the object multiplied by the fluid density times the added mass coefficient. For a surface ship at the surface this is also equal to the added mass coefficient times the body mass. Once an object is submerged however that is no longer true. A solid lead ball would have the same submerged added mass as a foam or hollow ball of the same size, even through the body mass is vastly different.

Furthermore, the sea floor consists of vastly different characteristics, dependent on location, geology and geophysics, depth, and water flow characteristics. The seabed can be flat or steep, hard or just an ooze that increases density with depth. Seabed formations that are swept by strong currents and / or storm waves are usually hard or composed of sand waves, or are bed plated by cobbles that are too large / heavy for the everyday water flows to sweep away. For some locations such as near the mouth of the Amazon river, the upper layers of the ooze like sediment are actually moving down stream at up to a knot (51 cm/s).

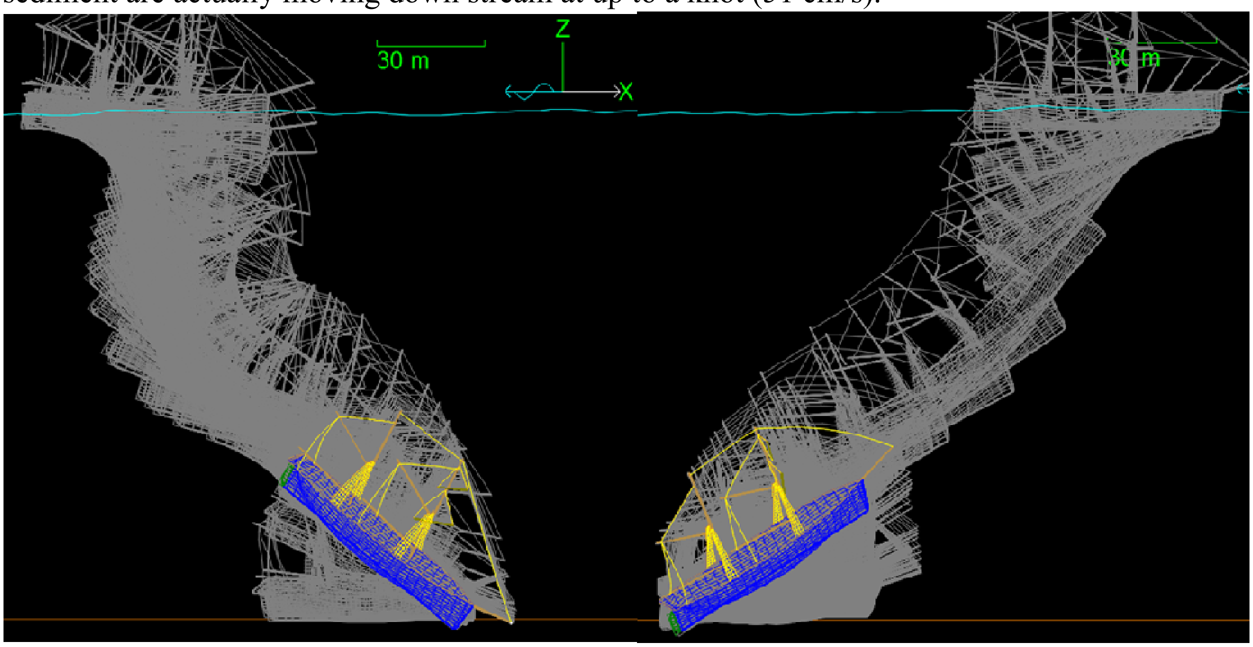

Figure 3: Same vessel sinking by the bow or by the stern

Figure 3 shows two illustrations of a vessel sinking and impacting the seabed. The only difference between the left panel where the vessel sank by the bow and the right panel where the vessel sank by the stern was the longitudinal separation between the centers of gravity and buoyancy on the hull. That's why it is critically important that the weights and centers of the vessel be established as closely as possible prior to making these analyses.

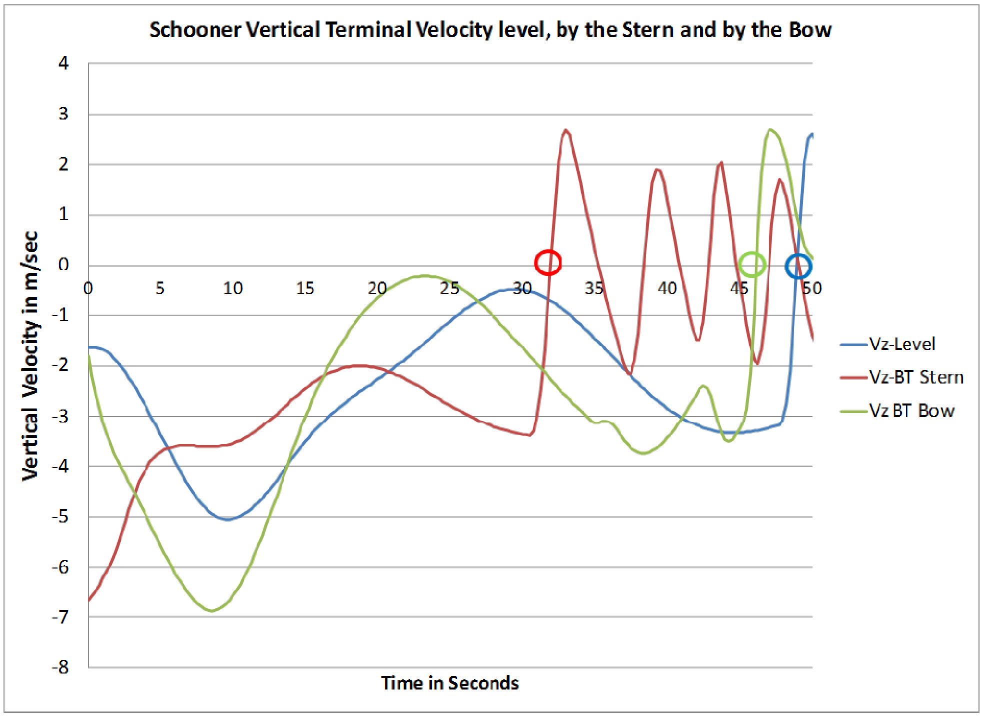

Figure 4: Schooner Vertical component of terminal velocity when sinking level, by the bow and by the stern.

Figure 4 shows the vertical components of the schooner's freefall to the bottom, when ballasted to sink level, by the bow and by the stern. The circles denote the zero crossing when the vessel strikes bottom. The bouncing after the initial impact is the other end coming down and some actual rebounding, which can be experienced by some vessels on some bottom types.

Another very important item that can be seen in figure 3 is that when a vessel strikes the bottom bow or stern first, some collision damage to that part of the hull is likely. .Evidence of such damage can actually be diagnostic when examining a wreck. A wreck that shows more damage at the bow than the stern most likely struck bow first. The end that settled last may have landed much more gently.

Bottom impact can cause substantial forces on objects within a vessel and can even initiate additional structural failures or objects being ejected into the debris field on impact.

In figure 4, the vessel is shown in the program to bounce a bit as it settles on the seabed. This can be controllable by setting the friction & damping coefficients of each object, the hardness of the bottom and the compressibility of the vessel.

If the hull of a vessel is modeled as a single entity, then the whole unit will have to be modeled as having the same crush properties. It is possible to build up the vessel model by attaching multiple 6 degree of freedom buoys together, each with different mass properties and crush parameters if necessary.

In figure 3, the position of the impact point shows that the impacting object gouges the bottom, forming a crater. In some cases, the vessel comes to rest covering this initial impact scar. The size, shape and orientation of the impact scar can also be diagnostic in the study of the wreck and the associated bottom impact damage.

The forces created upon impact, however, partially depend on the vessel's characteristics. For wooden sailing vessels with lots of masts, spars, standing rigging, running rigging and sail cloth above the hull to slow it down, the impact velocity can be as little as a few feet per second. For an armored ship like the DKM *Bismarck*, the FS *Bouvet*, or the USS *San Diego*, the impact velocity may be 25 to 30 knots. The Bouvet struck the bottom so hard and so fast that the stern drove itself into the bottom and the bow remains sticking out of the bottom at a significant angle, even now 100 years later. (Kolay et al, 2013)

The DKM *Bismarck* struck the unconsolidated sediment on the side of a seamount so hard that the bottom was crushed upwards by about one deck level. The water inside the flooded hull was violently compressed and vented out everywhere that there was a hole in the hull. Areas without a nearby hole were compromised at the weakest local structure, which was the joint between the 1/2 inch bottom plating and the much thicker armor belt. The forces and pressures acting at this location resulted in the tearing of jagged vents outwards along the seam. The waviness of the edge indicates that some stretching occurred with the tearing and the plastically deformed edge was too long to return to a straight line, so a ripple occurred. (Cameron & Garzke et al, 2008) The unconsolidated sediment layer under *Bismarck* liquefied on impact and acted as a partial bearing that allowed the ship to slide approximately 1500m down slope before it finally came to rest.

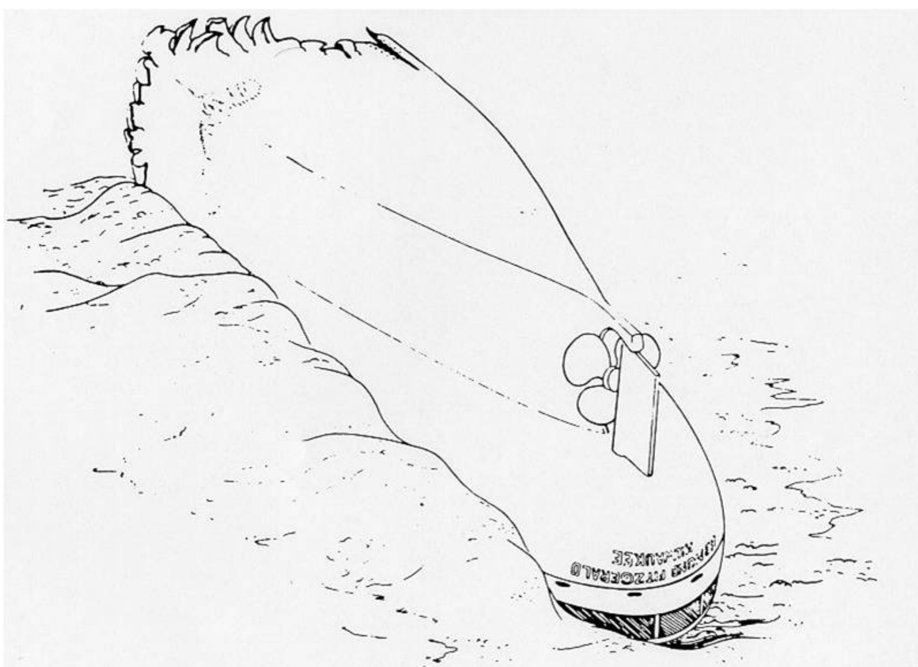

Figure 5: Illustration from USCG Report, *Edmund Fitzgerald* Stern with Sediment Dune to the Left

Some of the impact inertia of a vessel transfers to the bottom material on impact and can plow up a significant dune of sediment and/ or leave a slide scar that is visible up to hundreds of years later. In other circumstances, the initial sediment shapes due to impact can be remolded and / or erased by scour during subsequent strong bottom water flow events. The stern section of the Edmund Fitzgerald shown in a US Coast Guard investigation sketch is in shown in figure 5.

Another frequent consequence of a large object making seabed impact is the creation of a large cloud of sediment that is ejected up into the water column.

There is a boundary layer and turbulent wake plume that follows an object as it plunges through the water column that will continue to impact the bottom for some seconds to minutes after the physical body has landed. This wake plume cannot pass through the bottom so it billows up in what looks like an atmospheric microburst, or an inverted mushroom cloud. This further dusts up the bottom material. The sediment mobilized by these effects will rain back down and, in a steady current, this sediment plume will be moved downstream as it falls. Sediment particles such as stones which have less drag area and greater weight will fall out of suspension in the near field. Small clay like particles may remain suspended for days and travel many miles before they come to rest. The more turbulence that is present in the flow field, the more material that will remain suspended, and for longer.

Post Deposition Velocity Field

Any object on the seabed is acted on by the local velocity field. The instantaneous velocity field is the vector sum of the different mean flows and any wave velocities that reach that depth. Figure 6 shows the results of the deep water wave equation, shown in the blue box, versus depth for a continuum of ordinary ocean wave periods for a 4m significant wave height.

The Orcaflex model solves the wave equation for whatever depth the user inputs and solves the full Morrison equation, which includes the effects of mass and added mass, as well as the drag equation. The key conclusion of figure 6 is that the longer period waves typical of local storms or that propagate into the area from distant storms, stir the water column much more than the shorter period waves associated with locally generated wind chop.

The velocity field affects an investigation in 3 ways. First, how did it figure into what happened to cause the sinking and deposition mechanics? Second, what has it done to objects on the bottom at different stages of the wreck decomposition? Third, how must it be considered when planning an expedition to the site?

For depths deeper than about 500 meters, the effect of surface waves can be neglected, except for planning site visits where they will mean the difference between launching the equipment and taking a weather day. Contrastingly, long period swells can still have appreciable velocity several hundred meters below the surface.

Areas such as the north shore of the Hawaiian Islands see long period swells on a regular basis due to the long fetch and relatively steep drop off to full oceanic depths near shore. Areas such as much of the US East Coast, have a long continental shelf and short fetch from the west, where the weather patterns typically come from. Long period swells, with more than a negligible height, are unusual on the US East coast unless there is a hurricane or other severe storm passing offshore.

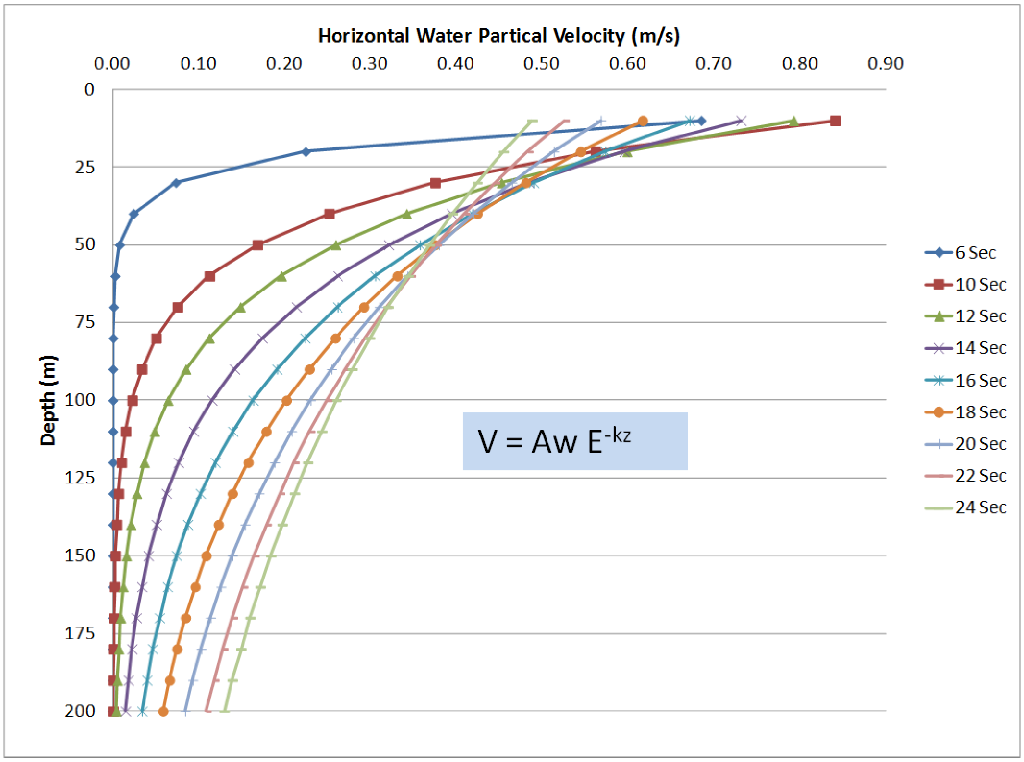

Figure 6: Wave Particle Motion Decay with Depth

Some areas have strong tidal currents and a large tidal range, whereas others have very little of either. Even deep water sites with normally quiescent current conditions, can be visited by benthic storms that create a High Energy Benthic Boundary Layer (HEBBLE) event with bottom velocities of 1.5 to 2 knots. (Gross, Williams & Nowell, 1988) & (Nowell, Holister & Jumar, 1982)

The prudent investigator makes a study of the conditions in the area where the wreck is known or suspected to have occurred. Likewise any local NOAA/NDBC or other weather buoys should be consulted to determine what the typical and extreme wave climatology is likely to be. For areas of the world where no buoy data is available, other methods must be used to approximate the wave and current climatology. (Kery et al, Guidelines chapters 43,44,45. 2012)

Initial Debris Field Creation

The initial debris field is created in the course of the sinking and over the next several hours if large area light weight objects, that fall slowly, are involved.

A group of everyday objects in the form of luggage were released at the surface in storm waves and allowed to freefall independently to the bottom, in an OrcaFlex model

Table 1: Typical Debris Field Objects

Item Description	Length	Width	Height	Thickness	Volume	Weight	Weight
	inches	inches	inches	in	in^3	Pounds	Pounds
Carpet Bag 1	12	6	9	0.0625	29.25	1.36	15
Carpet Bag 2	18	8	12	0.0625	57.00	2.65	20
Carpet Bag 3	24	11	16.5	0.0625	105.19	4.89	25
Carpet Bag 4	30	14	21	0.0625	168.00	7.80	40
Carpet Bag 5	36	16	24	0.0625	228.00	10.59	70
Steamer Trunk 1	12	18	14	0.1875	238.50	11.08	40
Steamer Trunk 2	30.5	17	21	0.1875	568.50	26.41	80
Steamer Trunk 3	32	19	21	0.1875	629.63	29.25	90

	Face	End	Bottom	Face	End	Bottom								
	Cd	Cd	Cd	Area	Area	Area	CGx	CGy	CGz	CBx	CBy	CBz	Volume	Weight
				m^2	m^2	m^2	m	m	m	m	m	m	m^3	tonnes
Carpet Bag 1	0.9	1.05	1.05	0.073	0.021	0.016	0.152	0.076	0.076	0.152	0.076	0.111	0.000	0.007
Carpet Bag 2	0.9	1.05	1.05	0.139	0.037	0.093	0.229	0.102	0.102	0.229	0.102	0.152	0.001	0.009
Carpet Bag 3	0.9	1.05	1.05	0.255	0.070	0.170	0.305	0.140	0.140	0.305	0.140	0.210	0.002	0.011
Carpet Bag 4	0.9	1.05	1.05	0.405	0.114	0.271	0.381	0.178	0.178	0.381	0.178	0.267	0.003	0.018
Carpet Bag 5	0.9	1.05	1.05	0.557	0.149	0.372	0.457	0.203	0.203	0.457	0.203	0.305	0.004	0.032
Steamer Trunk 1	0.9	1.05	1.05	0.108	0.093	0.139	0.152	0.229	0.119	0.152	0.229	0.178	0.004	0.018
Steamer Trunk 2	0.9	1.05	1.05	0.413	0.138	0.335	0.387	0.216	0.178	0.387	0.216	0.267	0.009	0.036
Steamer Trunk 3	0.9	1.05	1.05	0.434	0.154	0.392	0.406	0.241	0.178	0.406	0.241	0.267	0.010	0.041

The unit conversions between the upper and lower table are necessary to use the default units in the software. The terminal velocities achieved ranged from unsteady values of 0.6 to 4.8 m/s. (1.2 to9.3 knots) The variation with time for any of the objects is due to waves near the surface and tumbling such that different areas were exposed to the flow at different times. When a larger drag area is exposed to the direction of travel, the object slows down and when a smaller aspect is exposed it speeds up.

Each of the objects was input with the correct weight, buoyancy, and drag areas in each of 3 principle directions. They were released in currents and waves. Heavier objects with relatively small drag areas fall faster and travel less distance downstream due to the currents and waves. Larger light objects fall slower so the current in each layer has longer to act on them and they are able to drift further.

The drag areas used in a simulation and the sizes and shapes used in the graphics are separate inputs in OrcaFlex. In figure 7 all of the objects describes in table 1 were shown as 5m cubes, each with a different color so that they were visible at the scale of the illustration. Initially they were modeled with the graphics at real size and they were too small to see at this scale. Increasing the graphics size has no effect on the physics of the model, just on how hard or easy it is to visualize.

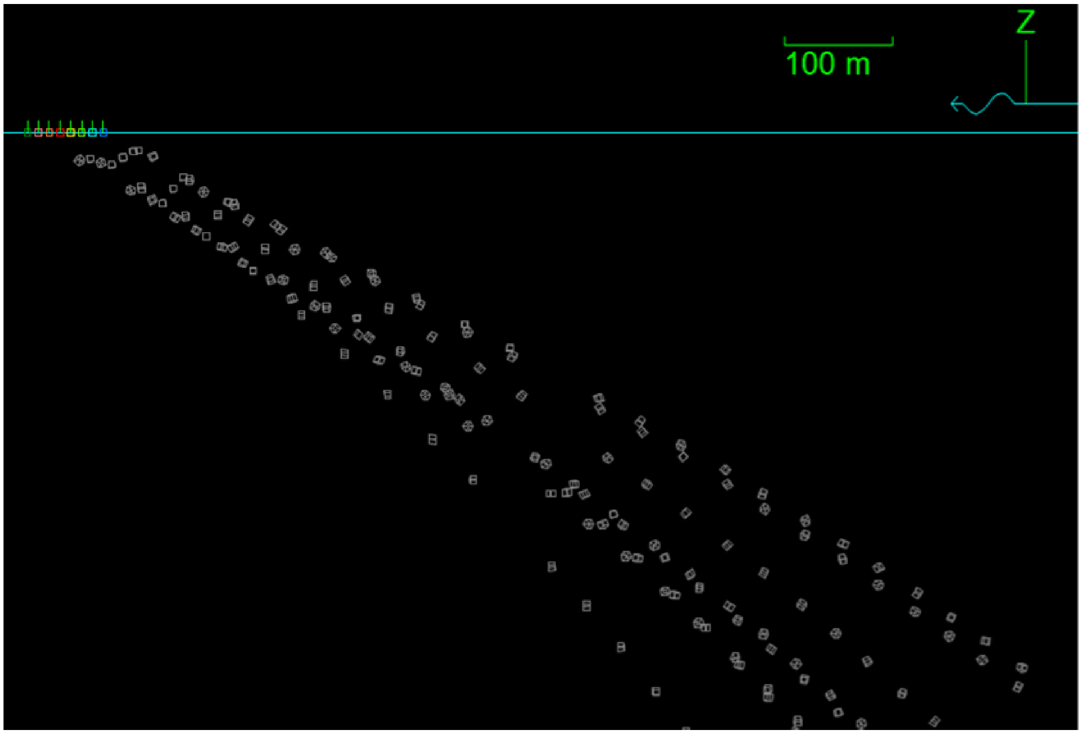

Figure 7: Fall of Debris Field object visualization in OrcaFlex

Similar analyses have been performed by the author for taconite pellets and for anthracite coal chunks in support of specific sinking analyses. Anthracite coal forms a diagnostic part of the debris field on several wrecks that the authors have studied. Taconite pellets were the iron ore cargo of the Edmund Fitzgerald, and the order in which the different hull sections reached the bottom could be determined by the distribution of the taconite pellets.

Velocity Acting on Sea Bed Objects

Figure 8 shows the physical situation where the water flowing from left to right is trying to push the Blocks A and B downstream. The blocks are held in position by a "friction" force that is often expressed as a coefficient Mu times the net downward force which is the weight (W) minus the buoyancy (B) of the object.

$$Holding\ power = (W - B) * Mu$$

This equation works well for dry objects on a dry, hard flat surface. Underwater, the "friction" term is more complicated because the surface is not necessarily hard or flat and because some objects, like B, are partially embedded in to the sea bed. The bottom is illustrated here as a series of sand waves which form roughly perpendicular to the prevailing flow direction.

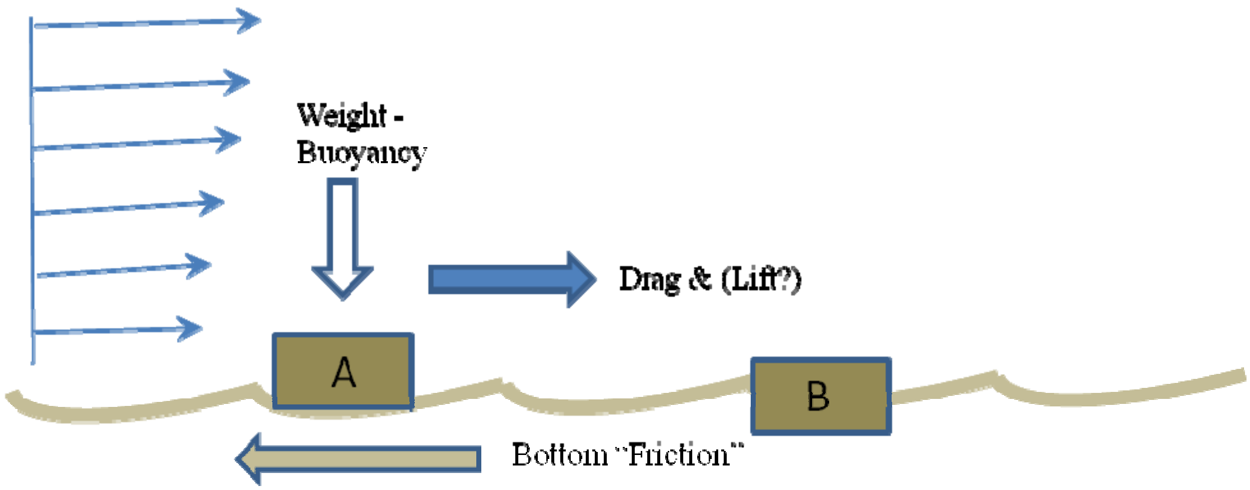

Figure 8: Definition Sketch for Bottom Friction Model

For deep sea buoy mooring anchors the "friction" coefficient has been calculated to include the mooring line tension lifting up. On the WHOI, MLML and BioWatt Moorings, that had in-line tension recorders, the friction coefficient has been determined to be as high as 5.0 (Kery Unpublished 1) for cast steel cylindrical clump weights (approx 10,000 pounds) in abyssal plain sediment at depths of 3000 to 5000 meters.

For normal objects, values of 0.5 to 0.75 are typical on hard sand bottoms. (Rocker 1990). For objects that must push a wedge of sediment out of the way to get free, the holding power is related to the weight of the wedge of sediment which varies by sediment type. The cohesiveness of the soil is also an important factor that varies from nil for sand and gravel to quite strong for some consolidated clays.

The OrcaFlex software can output a time series of the 3D velocity at any given point in the global modeling space, which can be used to visualize how the flow due to waves and currents will act on any given object.

The steady flow field also experiences a boundary layer effect near the bottom that follows a roughly logarithmic decay function. However oscillatory flows due to storm waves are less effected by boundary layer attenuation because they are not steady in one direction for long enough for a quasi-stable boundary layer to form.

An object on the seabed has a center of drag that is above the seabed that will cause an overturning moment. Most objects are asymmetric and have different drag areas and coefficients based on their orientation to the flow. The trails left on the surface of the sediment show that some objects will slowly drag downstream and may wobble side to side or tumble in the process.

Significant portions of the seabed materials can be stirred up into the water column by a passing storm and one would presume that anything lying there would likewise be mobilized. On one of the Globec cruises to the Georges Bank area a Mockness plankton tow conducted tens of meters above the seabed of the Great South Channel came back on board with about a gallon can worth of sand in it. The tow had never approached the bottom but the water was stirred up enough that the relatively coarse material had not fallen out of suspension yet.

The precise level of steady or oscillating flow necessary to move or tumble any specific object is unknown and determining it would probably require systematic testing, or the gathering of anecdotal information that could be quantified.

Figure 9 shows our generic topsail schooner on the bottom at a depth of 100m The grey shadows are the paths traveled by the masts, rigging, and hull due to a steady current and the action of storm waves passing overhead.

A set of 18 runs, each 10 minutes real time duration, were made to create illustrations of the motion resulting from this case and to examine the current and wave induced loads acting on the wreck. For a real analysis a longer time series would be necessary for statistical stability, but in this case that level of finesse was not warranted. The 18 runs took about an hour to set up in batch mode, another hour to run on a modest PC and then more hours to study the output data. It took about one man week of work to develop the hull form, weights and displaced volumes for all of the components and the rigging as far as is shown.

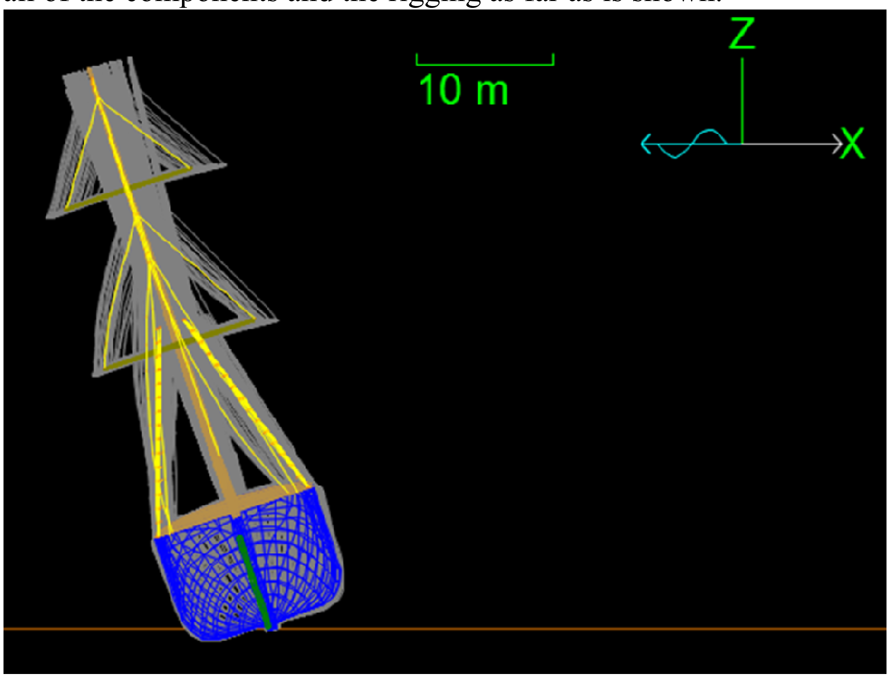

Figure 9: Orcaflex Model Of Typical Schooner Rocking On The Bottom Due To Storm Waves Passing Above.

The first set of runs in Table 2 shows a pairing of the rigging status between masts and spars only (M&S) and masts and spars with standing rigging as shown (W/SR). A 1/7th power curve was implemented for the current in set 1 which varies from 2 knots at the surface to 1 knot at the bottom. The waves are all coming toward the beam of the vessel in all cases. In the first two runs, the waves and currents are both oriented in the same direction. The second pair of runs was made with the current set to zero, while the third pair was modeled with opposing waves and currents. To model these waves, the JONSWOP spectrum was chosen as typical for storm conditions. (Ochi 2002)

Set two focuses on the effects of changing the wave modal period from steep waves with an 8 second period to longer swells with a 15 second period. The difference between the JONSWOP and a more typical Bretschneider Spectrum (ISSC) is shown between set 2 runs 2 and 3. Additionally, set 2 runs 3 through 6 show the effect of increasing the significant wave height in 1 meter increments.

Table 2: Schooner Bottom Runs Matrix

Run Number	Depth m	Rigging Status	Surface Current			Bottom Current			Current Decay	Sea State	H1/3 m	Tm sec	Wave Direction	Wave Spectral
Set1			knots	m/s	deg	knots	m/s	deg	Method	Number				Type
1	100	M&S	2	1.03	180	1	0.51	180	1 7Pwr.	5	4	9.7	180	JONSWOP
2	100	W SR	2	1.03	180	1	0.51	180	1 7Pwr.	5	4	9.7	180	JONSWOP
3	100	M&S	0	0.00	180	0	0.00	N/A	1 7Pwr.	5	4	9.7	180	JONSWOP
4	100	W SR	0	0.00	180	0	0.00	N/A	1 7Pwr.	5	4	9.7	180	JONSWOP
5	100	M&S	2	1.03	180	1	0.51	0	1 7Pwr.	5	4	9.7	180	JONSWOP
6	100	W SR	2	1.03	180	1	0.51	0	1 7Pwr.	5	4	9.7	180	JONSWOP
7	100	M&S	2	1.03	180	1	0.51	180	1 7Pwr.	6	6	12.4	180	JONSWOP
8	100	W SR	2	1.03	180	1	0.51	180	1 7Pwr.	6	6	12.4	180	JONSWOP
9	100	M&S	0	0.00	180	0	0.00	N/A	1 7Pwr.	6	6	12.4	180	JONSWOP
10	100	W SR	0	0.00	180	0	0.00	N/A	1 7Pwr.	6	6	12.4	180	JONSWOP
11	100	M&S	2	1.03	180	1	0.51	0	1 7Pwr.	6	6	12.4	180	JONSWOP
12	100	W SR	2	1.03	180	1	0.51	0	1 7Pwr.	6	6	12.4	180	JONSWOP
Run Number	Depth m	Rigging Status	Surface Current			Bottom Current			Current Decay	Sea State	H1/3 m	Tm sec	Wave Direction	Wave Spectral
Set2			knots	m/s	deg	knots	m/s	deg	Method	Number				Type
1	100	W SR	1	0.51	180	0.5	0.26	135	1 7Pwr.	6	6	8	180	JONSWOP
2	100	W SR	1	0.51	180	0.5	0.26	135	1 7Pwr.	6	6	15	180	JONSWOP
3	100	W SR	1	0.51	180	0.5	0.26	135	1 7Pwr.	6	6	15	180	Bretschneider
4	100	W SR	0	0.00	180	0	0.00	N/A	1 7Pwr.	7	7	13	180	JONSWOP
5	100	W SR	0	0.00	180	0	0.00	N/A	1 7Pwr.	7	8	14	180	JONSWOP
6	100	W SR	0	0.00	180	0	0.00	N/A	1 7Pwr.	7	9	15	180	JONSWOP

Run Number	H1/3 m	Tm sec	Roll-Range deg
	H1/3		Roll-Range
Set1_Run_4	4	9.7	5.48
Set1_Run_10	6	12.4	4.97
Set2_Run_4	7	13	4.67
Set2_Run_5	8	14	6.66
Set2_Run_6	9	15	9.70

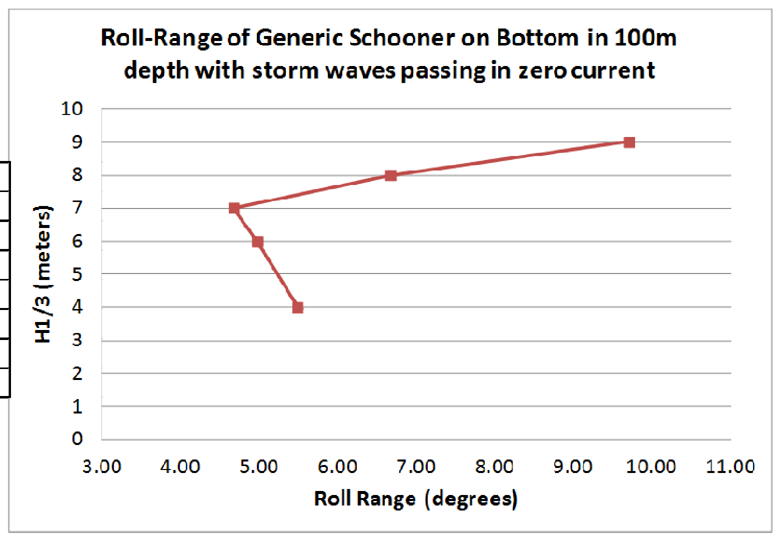

Figure 10: Roll Range as shown in Figure 7

Figure 9 shows the wreck rocking on the bottom due to waves. This motion accelerates hull decay, especially when rocks or other hard objects contact the hull. These oscillating loads can help the ship break apart over time.

Figure 10 shows the range of roll in the 600 second time series for 5 different significant wave heights. The fact that it does not appear to show uniform behavior with increasing wave height is not surprising. This is largely due to the short simulation duration. Note that the modal period of the wave spectra also increases with the wave height in this case. The short period run sees about 62 waves pass whereas the longer period only sees about 40. An ideal single run should probably see several hundred wave encounters to be statistically stable. This is trivial to accomplish but the much larger data files are more time consuming to work with and that was not warranted for this illustration case.

The wave model consists of 5 components, the spectral type, (Bretschneider, Ochi-Hubble, JONSWOP etc.), and then four that are expressed as a function of wave period which are, period, (typically several hundred to several thousand components), component amplitude, component direction of travel, and the starting phase. The statistics of the output spectrum should be the same for any input to the starting phase and the phases are usually set using a seeded random number generator. The seeded random number allows the phases to remain fixed for multiple cases and runs such that the results, although random, are wave for wave comparable. If the user resets the seed on the random number generator, a new "realization" in a completely different set of statistically identical waves will result. These new realizations have been shown to produce significantly different results in time series analyses.

This can be an important issue when you're trying to get a simulation to match a specific debris field feature. Changing the input wave phases to different random values will change the results and their statistics even though the input waves are statistically identical.

Dr. Armond Troesch and his students at the University of Michigan have developed a methodology whereby the spectral components making up the wave field can be made to all reach top dead center at a user selected instant in time which produces the largest possible wave. However there is a phase lag between the wave excitation and an objects response to it that is different for different degrees of freedom so the largest wave does not necessarily provoke the largest response. It is also possible by this method to mathematically create a wave that is too large / steep to actually exist in nature by exceeding the Miche breaking limit.

The connection moments of the masts and bowsprit about the hull are output by the software. The drag on each of the rigging lines is also calculated as an output. There are many different results data sets that can be directly extracted or reduced in post processing. What the investigator chooses to study is determined by the study goals. For this study of a fictitious vessel, the purpose of the study is to define the art of the possible and to learn what results can and cannot be expected and to what degree of fidelity. The type and quality of the data stream is important, the specific numerical values are only of qualitative interest.

Taphonomy of Seabed Objects

Two US Civil War era vessels of historical importance were chosen based upon prior work to discuss the effects of time on the bottom on the artifacts and debris field. The vessels selected are the USS *Monitor* which down flooded and sank in a storm December 31st, 1862, off Cape Hatteras, NC and the early submarine CSS *Hunley* which down flooded and sank February 17th, 1864 in the act of sinking the USS *Housatonic* at Charlestown, SC.

The *Hunley* was near shore in 8 meters of water until discovered in 1995. She was raised and conservation projects have been underway (Jacobsen, et al, 2012) in Charlestown ever since. There are holes attributed to erosion corrosion in several places where the water flows due to waves and currents acted to sand blast off the corrosion products that formed on the exposed surface of the metal. The sub was partially buried and the damage is at and above the mud line, which moved around some in the slightly over 100 years she was on/in the bottom.

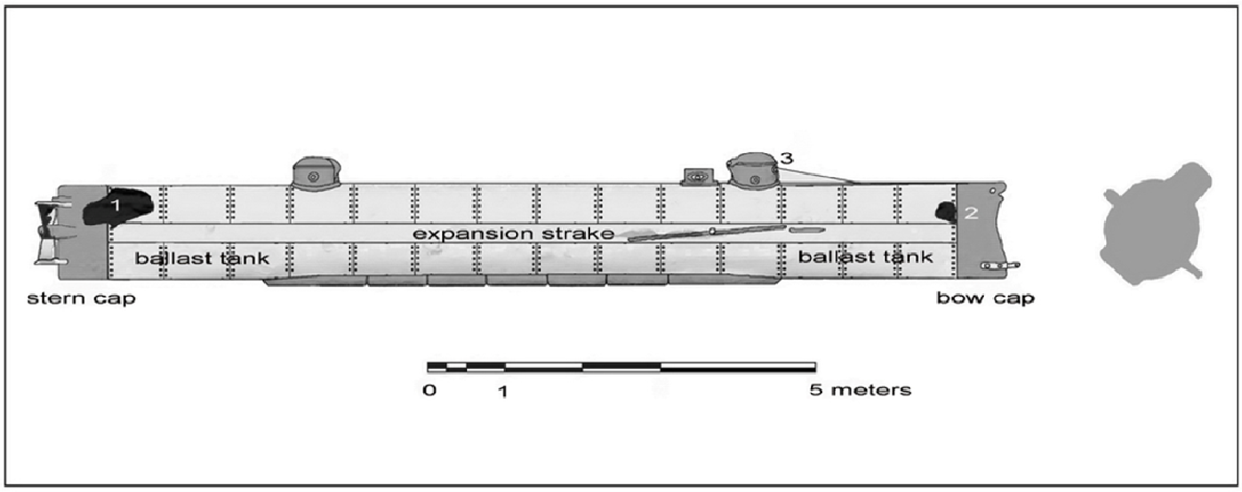

Figure 3. Drawing of the hull showing the location of hull breaches 1-3 and a cross section of the hull on the right. Structural components made of cast iron are highlighted dark gray.

Figure 11. Figure of CSS Hunley with caption from paper by Jacobsen et al, 2012

This erosion aggravated corrosion is a well known problem with the chains on buoy moorings as well. An inch and a half stud link chain will erode from new to less than 1/2 inch of material left in a year or so, but only for a few meters where the chain is continually moving on the bottom.

The *Monitor* was considerably deeper at 67 m, when it was rediscovered in 1973 and , therefore, saw less wave action than the Hunley, under normal circumstances. (Broadwater,2012) However the location off Cape Hatteras is frequented by the edge of the Gulf Stream with currents that can be in excess of 3 knots (154 cm/s)

The *Monitor* sat mostly proud of the bottom, upside down and resting on the turret. The turret, engine, propeller and other parts were later raised and are undergoing conservation at the Mariners Museum.

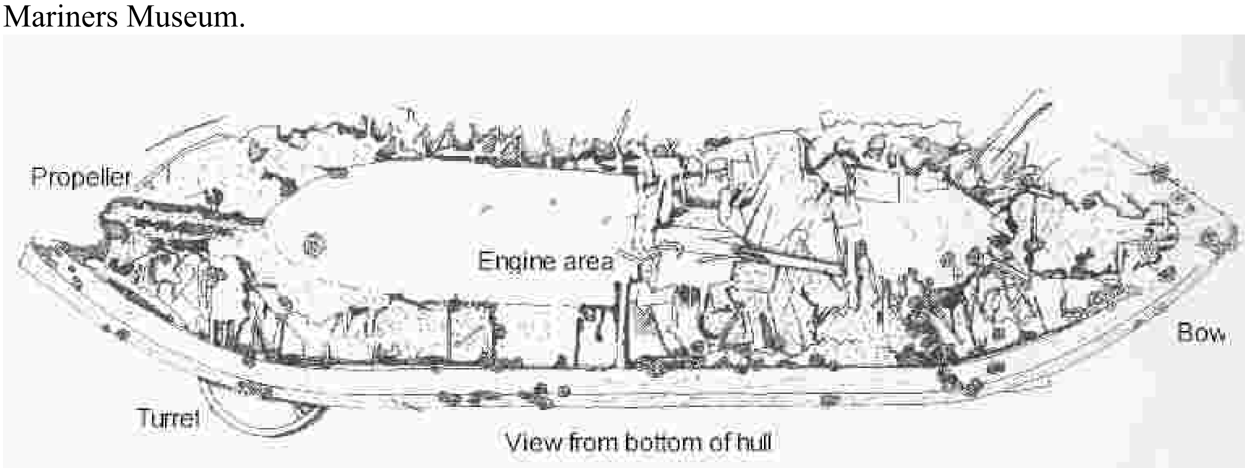

Figure 12: NOAA Sketch of *Monitor* as it was found on the bottom. Broadwater (2012)

Kery performed an Orcaflex analysis in 2012 on the Monitor and was able to re-create the vessel rolling over at the surface and the turret falling out followed by the model of the wreck landing inverted and on top of the turret, similar to how the wreck was found. (Kery et al (4)

2012) The taphonomy of the *Monitor* is tough to describe. The lower bottom, which landed uppermost, is mostly collapsed down into what was the interior of the vessel, but the causes of different portions of the damage are not well known. There is a possibility that the wreck was depth charged during WW II. The location has been swept by a number of severe hurricanes during the interval on the bottom which may have caused further damage, obscuring forensic evidence.

Accuracy and Limitations

"**All models are wrong, but some models are useful",** or so the saying goes. The methods of modeling described herein are useful in that they allow a first of its kind capability to investigate vessels and debris fields that have sunk recently or long ago. It is possible to postulate objects falling off at different depths, during the plunge or being advected on bottom impact, and then check the feasibility of those hypotheses by systematic modeling.

The modeling method is limited in accuracy by a number of internal and external factors.

External factors and limitations include

- The model requires that the weights and centers of gravity and buoyancy are known as inputs. For many vessels, especially historic or pre-historic vessels, only an approximate value is possible. This is discussed at length in (Kery (2) 2015).
    - Note that Pre-Historic in the context of old ships is any vessel for which sufficient drawings and technical data are no longer available in the open literature or via standard archive search techniques.
- For historic and pre-historic vessels, like many of the amphora wrecks found in the Mediterranean, the original and damaged conditions of the vessel that lead to the sinking are unknown. The use of historic vessels where witness accounts can help fill in that data, is necessary to further calibrate the methodology before it can be widely applied to vessels for which the conditions and reason(s) for sinking are unknown.
- While there are published values for the drag and added mass of many shapes, there is usually a lot of scatter in the data they were derived from. In any given case it's impossible to know the exact values that apply more accurately than perhaps within +/- 10 to even 20%.
- There is no published data on the drag of the superstructures of ships in most cases. While this can be approximated as a set of shapes, there is no way to get the blocking effects versus azimuth correct without a physical model and wind tunnel testing. Simplistic models used in the design of ship to pier, and ship to ship moorings offer some data, but the accuracy is very approximate. (NAVSEA 1987, OCIMF various, Seelig, 1999)
- The sea bed soil characteristics are usually not known to a level where they can be converted into the topography and soil properties that the OrcaFlex program can use for analysis.
- The materials of construction for steel ships are relatively easy to find and develop, but for wooden or composite vessels there can be a wide variation in material properties from type to type and from board to board within a material type. Oak for instance has a density variation of 40% or more from board to board and from one subtype of oak to another. The actual properties of each of the many different boards and timbers that make up a wooden vessel cannot be known exactly. Even if such a perfect knowledge existed on the day the ship was launched, the action of aging, dry rot, fungus attack, insect attack, water logging, and a host of other deteriorating factors, will render the true properties at the time of sinking largely unknown.

- The wave and current conditions that were occurring at the time of the wreck are rarely known to any level of fidelity. They can be approximated from existing data and for similar storms as Kery showed for the sinking of the USS *Monitor* and the SS *Edmund Fitzgerald* (Kery et al, 2012, Kery & Fisher 2012).
- For sailing vessels, the details of the masts, spars and rigging can only be approximately known.
    - Spars can be raised or lowered and the position at the time of sinking is mostly unknown.
    - The pretension on any given line is unknown so the dynamic tensions and vortex induced vibrations can only be approximated. The pretension plus the dynamic tensions play a very important role in determining the string natural frequencies and how close the vortex induced vibration frequencies is to the fundamental and higher modes. The drag coefficient can more than double under some circumstances.
    - Sails can be set or furled loosely or tightly to the spars. For set sails there is an abundance of data on the lift and drag properties. For sails that are furled, no drag area or drag coefficient data is known to the authors.

Internal limitations include

- The program does not change the flow characteristics due to the presence of an object. The flow is correctly modeled for the currents and waves at the X,Y,Z, time coordinate of any given point. The drag and mass related forces are calculated as well as the input data allows, but there are no shadowing or wake effects modeled.
- There is no built in capability to have objects release from one another except to use a network of links and geometry. This treats the links as if they have properties that must be modeled in the time series, making the solution mathematically unstable in some instances.
- The version of the Orcaflex Software that the authors have available can model a vessel navigating along a user defined path and responding to thrust and wing forces due to sails, rudders, keels, paddlewheels or propellers, but the side slip or "transfer" in a turn is not correctly modeled.

Concluding Remarks

This paper is part of a trilogy of papers, one describing the weights and centers estimation on historic ships was published at the Society of Allied Weights Engineers conference in May 2015. A companion paper that goes into greater depth on the sinking phase of the analysis has been submitted to the SNAME 2015 Annual meeting. This paper is more focused on the later steps after the objects have been deposited on the bottom.

Many additional analyses have begun or are in the planning stages. Each new ship modeled presents its own challenges and opportunities to further refine the techniques described herein.

A methodology whereby the software can be used to model progressive flooding is under investigation on one vessel.

A proposed analysis of the sinking of the *Pride of Baltimore 1*, would offer the opportunity to model and observe the effects of a ship that sank with some sails raised in a well documented manner. However a precise survey of the wreck on bottom is not known to the authors, and that would be necessary to validate and verify the analyses.

A proposed sinking model of the RMS *Titanic* could be used in concert with the latest debris field maps to settle some of the arguments concerning where and how different parts separated.

The replica sailing vessel *Bounty* that sank in hurricane Sandy would be an excellent wreck to study as the decay of the wooden structure could be studied across the progression from wooden ship to ballast pile. Unfortunately, no drawings have come to light that would allow the model to be created. Information from the original HMS *Bounty* is available but the replica was much larger and had different proportions.

A sailing warship the Mars has been found in Swedish waters dating from the 1500's. Fredriksson, (2015) Because of the brackish waters, which prevent most marine borers from reaching the wreck, much of the hull is still intact. While this offers some promise, the bow of the ship was destroyed by an explosion that lead to the sinking and that would certainly complicate the analysis.

There are ample opportunities for further research projects associated with this type of analysis. Many universities have existing facilities that could shed useful light on much of the missing data with sufficient accuracy to support an undergraduate senior capstone project or masters or PhD thesis project.

The authors hope that these types of analyses will become useful to a wider cross section of investigators of casualties at sea, as an aircraft intact or in pieces can be modeled as readily as a ship or any other type of manmade object.

Acknowledgements

The authors would like to thank Computer Sciences Corporation, (CSC) for allowing us to continue to use these powerful tools, outside of work hours in the pursuit of this fascinating research. Kery would especially like to acknowledge the inspiration and support of the CSC Distinguished Engineers program which has made publishing and presenting these papers possible.

References

Bass, G.F., “1975 Archaeology Beneath the Sea, A Personal Account”; 1975 Walker and Company New York.
Bass, G.F., et al, “2005 Beneath the Seven Seas; Adventures with the Institute of Nautical Archaeology”; 2005, Thames & Hudson, London.
Broadwater, John D., *USS* Monitor*: A Historic Ship Completes Its Final Voyage*. College Station, TX: Texas A&M University Press, 2012.
Cameron, J., Dulin R.O. Jr., Garzke, W.H. Jr., .Jurens, W., Smith, K.M.Jr., "2008 The Wreck of the *DKM Bismarck*, A Marine Forensic Analysis"; Presented at the SNAME annual Meeting 2008
Faulkner, Douglas, "1998 An Independent Assessment of the Sinking of the *MV Derbyshire*", SNAME Transactions VOL 106, 1998, pp59-103
Fredriksson, M., "The skeletal remains of the naval ship Mars" Bachelor's thesis, 15 ECT’s, spring 2015 Uppsala University Sweden, Campus Gotland, Department of Archaeology and Ancient History
Gross, T.F., Williams, A.J.III., Nowell, A.R.M, "A Deep sea Sediment Transport Storm"; Nature, 331, 518-521, Feb 1988
Hoerner, S.F., "1965 Fluid-Dynamic Drag"; Published by the Author 1965
Hoerner, S.F, Borst, H.V., "1975 Fluid-Dynamic Lift" Published by the Author 1975
Jacobsen M., Blouin, V.Y., Shirley, W., "Does Erosion Corrosion Account for Intriguing Damage to the Hull of the Civil War Submarine *H.L. Hunley*? 2012 International Marine Forensics Symposium
Kery, S.M., "On the Hydromechanics of Vessels and Debris Fields During Sinking Events"; submitted to SNAME Annual Meeting November 2015 in Providence RI
Kery, S.M., “Weights Engineering of Historic Vessels": Presented at SAWE International Symposium, Alexandria, VA, May 2015
Kery, S.M., et al, “Guidelines for Marine Forensics Investigations”; (Book, 46 chapters approx. 700 pages), Kery S. Editor and principle author (Chairmen MF-8 Panel / Editor) Published as SNAME T&R Bulletin 8-1, April 2012
Kery, S., Eaton, M., Quigley, C., Henderson, S., Broadwater, J., Johnston, J., Krop, D., Nordgren, E., Vada, T.”A Forensic Investigation Of The Sinking Of USS *Monitor* Using Modern Naval Architecture Tools And Technologies”; 2012 International Marine Forensics Symposium, April 2012
Kery, S.M., Fisher, B.,”A Forensic Investigation Of The Breakup And Sinking Of The Great Lakes Iron Ore Carrier *Edmund Fitzgerald*, November 10th 1975, Using Modern Naval Architecture Tools And Techniques”; 2012 International Marine Forensics Symposium, National Harbor MD, April 2012
Kolay,S., Taktak, O., Karakas, S., Atabay, M., "Echos from the Deep, Wrecks of the Dardanelles Campaign";2013, published by the Ayhan Sahenk Foundation, Istanbul, Turkey.
NAVSEA DDS 582-1, “Calculations for Mooring Systems”, 1987
OCIMF Mooring Equipment Guidelines, 1st, 2nd and 3rd editions
NFESC Technical Report TR-6012-OCN, “U.S. Navy Heavy Weather Mooring Criteria”, William P. Seelig, P.E. March 1999

Nowell, A.R.M., Hollister, C.D., Jumars, P.A.," High Energy Benthic Boundary Layer Experiment (HEBBLE)"; EOS Transactions of the American Geophysical Union, Aug, 1982
Ochi, M.K., "Hurricane Generated Seas"; Elsevier 2003
Pattison, J.N., Rispin, P.P., Tsai, N.T., " Handbook of Hydrodynamic Characteristics of Moored Array Components", David W. Taylor Naval Ship R&D Center report No. SPD-745-01, March 1977
Rocker, Karl, Jr., "Marine Geotechnical Engineering"; March 1985, Report AD-A157-894, Naval Civil Engineering Lab, Port Hueneme, CA.
Steffy, J. Richard, (1994 *Wooden Shipbuilding and the Interpretation of Shipwrecks"*, College Station: Texas A&M University Press, 1994
Tanner, Pat, "Digital Reconstruction and Analysis of the Newport Ship"; Newport, South Wales, UK, 2013
Tanner, Pat, "3D Laser Scanning for the Digital Reconstruction and Analysis of a 16th-Century Clinker Built Sailing Vessel"; (Drogheda Ship), 2013 Underwater Archaeology Proceedings
Throckmorton, P., Editor, "The Sea Remembers, Shipwrecks and Archaeology"; 1987, Weidenfeld & Nicolson, New York.